

General Disclaimer

One or more of the Following Statements may affect this Document

- This document has been reproduced from the best copy furnished by the organizational source. It is being released in the interest of making available as much information as possible.
- This document may contain data, which exceeds the sheet parameters. It was furnished in this condition by the organizational source and is the best copy available.
- This document may contain tone-on-tone or color graphs, charts and/or pictures, which have been reproduced in black and white.
- This document is paginated as submitted by the original source.
- Portions of this document are not fully legible due to the historical nature of some of the material. However, it is the best reproduction available from the original submission.

NASA Contractor Report 156855

M2, S2, K1 Models of the Global Ocean Tide of an Elastic Earth

(NASA-CR-156855) M2, S2, K1 MODELS OF THE
GLOBAL OCEAN TIDE Final Report (National
Oceanic and Atmospheric) 36 p HC A03/MP A01
CSCL 08C

N79-30907

G3/48 Unclass
31855

M. E. Parke

and

M. C. Hendershott

August 1979

NASA

National Aeronautics and
Space Administration

Wallops Flight Center

Wallops Island, Virginia 23337
AC 804 824-3411



1. INTRODUCTION

Many problems in geophysics involve different areas of investigation which are interrelated. One such problem is investigation of phenomena at tidal frequency in the solid earth and ocean. On the one hand, ocean generated tidal signals are present in many geophysical measurements, such as those of satellite elevation, gravity, tilt, and strain. On the other hand, the ocean tide is affected by the elastic properties of the solid earth, and so accurate modeling of the ocean tide depends on knowledge of the solid earth.

In order to make full use of geophysical data, geophysicists and geodesists need realistic models of the open ocean tide. But knowledge of the ocean tide has been difficult to obtain because ocean basins are close to resonance at tidal frequencies. This makes accurate modeling of the ocean tide difficult. It is the purpose of this paper to present models of the M₂, S₂, and K₁ tides that were developed to provide a first order correction to the problem of resonance. To facilitate the use of these models by geophysicists, maps of the geocentric tide, the induced free space potential, the induced vertical component of the solid earth tide, and the induced vertical component of the gravitation field are presented. These fields were calculated with Green's functions provided by W. E. Farrell (private communication).

2. THE PROBLEM

Laplace's Tidal Equations (LTE) may be written in negative mercator coordinates as

$$u_t - (2\Omega \tanh\tau)v = -g(\zeta - \Gamma/g)_\phi / a$$

$$v_t + (2\Omega \tanh\tau)u = -g(\zeta - \Gamma/g)_\tau / a$$

$$(\zeta_t - \delta_t) + ((uD)_\phi + (vD)_\tau) / a \operatorname{sech}^2\tau = 0$$

where (τ, ϕ) are the mercator latitude and longitude, (u, v) are the corresponding velocities, ζ is the geocentric ocean tide, Γ is the total tide generating potential, δ is the geocentric solid earth tide, D is the local depth of the ocean, a is the radius of the earth, and Ω is the earth's angular rate of rotation. $\tau = -2\lambda \tan(\pi/4 - \theta/2)$ where θ is latitude.

Introducing the observed tide $\zeta_0 = \zeta - \delta$ and writing

$$\zeta_0(\phi, \tau, t) = \operatorname{Re}\{\zeta_0(\phi, \tau)e^{-i\sigma t}\} \quad \text{etc.}$$

allows LTE to be written as

$$-i\sigma u - (2\Omega \tanh\tau)v = -g(\zeta_0 + \delta - \Gamma/g)_\phi / a$$

$$-i\sigma v + (2\Omega \tanh\tau)u = -g(\zeta_0 + \delta - \Gamma/g)_\tau / a$$

$$-i\sigma\zeta_0 + ((uD)_\phi + (vD)_\tau) / a \operatorname{sech}^2\tau = 0.$$

Solving for u and v , and placing these results back into the continuity equation yields

$$\mathcal{L}(\zeta_0) + \varepsilon^2 \operatorname{sech}^2\tau \zeta_0 = \mathcal{L}(\Gamma/g - \delta)$$

where

$$\begin{aligned} \mathcal{L} = & QH\nabla^2 + [(QH)_\phi - (i/s)(QH \tanh\tau)_\tau] \partial_\phi \\ & + [(QH)_\tau + (i/s)(QH \tanh\tau)_\phi] \partial_\tau \end{aligned}$$

$$\epsilon^2 = 4\Omega^2 a^2 / g D_0$$

$$Q = 1 / (s^2 - \tanh^2 \tau)$$

$$D = D_0 H(\phi, \tau)$$

$$s = \sigma / 2\Omega.$$

For a rigid earth, $r = U$ (the astronomical potential), and $\delta = 0$. In the presence of solid earth deformation and self-gravitation by the water column, $r/g - \delta$ may be expressed after Hendershott (1972) as

$$r/g - \delta = \sum_n (1 + k_n - h_n) U_n / g + \iint \zeta_0(\phi', \tau') G(\phi, \tau / \phi', \tau') \operatorname{sech}^2 \tau' d\tau' d\phi',$$

where $G(\phi, \tau / \phi', \tau')$ is a Green's function constructed by Farrell (1972), (k_n, h_n) are appropriate Love numbers (Munk and McDonald, 1960), and U_n is the n -th spherical harmonic of U .

Thus the final equation becomes

$$\begin{aligned} \mathfrak{L}(\zeta_0) &\equiv \mathfrak{L}[\zeta_0 - \iint_{\text{oceans}} \zeta_0(\phi', \tau') G(\phi, \tau / \phi', \tau') \operatorname{sech}^2 \tau' d\tau' d\phi'] + \\ &\epsilon^2 \operatorname{sech}^2 \tau \zeta_0 = \mathfrak{L}[\sum_n (1 + k_n - h_n) U_n / g]. \end{aligned}$$

We call this the elevation equation. Regardless of boundary conditions and regardless of the (numerical) procedure used to invert the operator \mathfrak{L} , the presence of the global integral in the above equation makes solution difficult.

All this paper's models specify the observed tide at the computational boundaries, as in Hendershott (1972). The models are frictionless but energy dissipation is obtained by allowing energy to flow through the computational boundaries, thus modeling energy flow into shallow marginal seas and shelves.

Hendershott (1972) proposed the iterative sequence

$$\mathcal{L}(\zeta_0^{(1)}) + \epsilon^2 \text{sech}^2 \zeta_0^{(1)} = \mathcal{L}[\sum_n (1+k_n-h_n)U_n/g]$$

$$\mathcal{L}(\zeta_0^{(i)}) + \epsilon^2 \text{sech}^2 \zeta_0^{(i)} = \mathcal{L}[\sum_n (1+k_n-h_n)U_n/g + \iint_{\text{oceans}} \zeta_0^{(i-1)} G \text{sech}^2 \tau' d\tau' d\phi']$$

and found it to be divergent for M2 in the absence of interior dissipation. Gordeev, et al. (1977) showed that this procedure will converge in the presence of interior dissipation.

Parke (1978) used iterates $\zeta_0^{(i)}$ generated as above to provide a basis set for a least squares solution to the dissipationless equations. The iterative procedure was restarted periodically to avoid redundancy in the $\zeta_0^{(i)}$. These least square solutions, however, proved unrealistically resonant for the semi-diurnal constituents M2 and S2. None of the solutions conserved mass, even that for K1 (which compared favorably with island data). This is an important liability for geophysical calculations, as was shown by Farrell (1972a).

The difficulty with being near resonance is that small errors in how one's model represents the real ocean cause small errors in the frequencies at which the model basin resonates. Far from resonance, these errors should have a correspondingly small effect on the model tide. Near-resonance, however, these small errors cause significant errors in the amplitudes of near resonant modes, and consequently cause significant variations in the model tide. Even relatively small changes in basin parameters, such as the mean depth of the ocean, cause significant changes in the represented tide near resonance.

In a one mode system, i.e., one where a single near-resonant mode dominates the solution, the amplitude of the mode can be adjusted by varying a single parameter such as the mean depth. A good example of this is the model of the Gulf of California by Stock (1976), where empirically choosing this single parameter improves the model dramatically. Unfortunately, the global tide appears to be a multi-mode system, and so adjustment of the tidal elevation field via a parameter search would require at least two and most likely more parameters. As the cost of such a search depends quite strongly on the number of parameters used, this approach could prove quite expensive.

An alternate method for adjusting the amplitude of near resonant modes is given in the next section.

3. A DYNAMIC INTERPOLATION OF ISLAND DATA

The test functions $\zeta_0^{(i)}$ used by Parke (1978) to solve LTE in the presence of tidal loading may be regarded as linearly independent combinations of the eigenmodes of the discretized tidal operator \mathcal{L} . We have generated a representation of the actual ocean tide by using these test functions to interpolate between island data in the least squares sense. If we believe that the modifications of our finite difference operator which are necessary to make its near tidal resonant frequencies the same as those of the real ocean would have but small effect on the spatial shape of the corresponding eigenmodes, then this least squares fit closely approximates the solution of that modified finite difference model.

The least squares fit $\hat{\zeta}_0 = \sum_{i=1}^n A_i \zeta_0^{(i)}$ is obtained by solving

$$(\partial/\partial A_j) \left\{ \sum_{I=\text{islands}} \left| [\zeta_I - \sum_{i=1}^n A_i \zeta_0^{(i)}(\phi_I, \tau_I)] \right|^2 \right\} = 0, j=1, n$$

for the weights A_i . Here ζ_I is the tide at island I.

The test functions $\zeta_0^{(i)}$ each separately reproduce the specified boundary tides. Requiring $\sum_{j=1}^n A_j = 1$ forces $\hat{\zeta}_0$ to also reproduce them. The test functions $\zeta_0^{(i)}$ do not individually conserve mass, i.e.,

$$\bar{\zeta}_0^{(i)} = \left\{ \iint_{\text{oceans}} \zeta_0^{(i)}(\phi, \tau) \operatorname{sech}^2 \tau d\tau d\phi \right\} / \{\text{area of oceans}\} \neq 0.$$

Requiring $\sum A_j \bar{\zeta}_0^{(j)} = 0$ forces $\hat{\zeta}_0$ to conserve mass.

For the M2 fit, $n=24$ iterates were used, for S2, $n=16$ and for K1, $n=8$. The fits presented below were obtained requiring $\sum_{j=1}^n A_j = 1$ (although $\sum_{j=1}^n A_j$ came out within a few percent of unity when this constraint was not imposed). $\sum_{j=1}^n A_j \bar{\zeta}_0^{(j)} = 0$ was likewise required although it also tended to be small (less than .1 cm for all three constituents when unconstrained). We do not entirely understand why $\hat{\zeta}_0$ thus conserves mass so well while the least squares solutions to the finite difference elevation equation, with the same boundary conditions, do not ($\sum_{j=1}^n A_j \bar{\zeta}_0^{(j)}$ was several orders of magnitude larger for the least square solutions even when the mean depth was intentionally altered simply to avoid resonance).

Least squares fits using different sets of M2 test functions generated over a range of 5% in the mean depth yield essentially the same elevation fields. This occurs even though the different sets of test functions differ markedly. We regard this latter point as qualitative confirmation of our belief, expressed above, that changes in the spatial shapes of the eigenmodes of the tidal operator are not a major source of error in our calculations.

Island tide gauges tend to be in the worst possible places, i.e., inside lagoons. This problem can cause a bias in the generated elevation field. To get an idea of this bias, seven islands in the Pacific were empirically corrected for near station phase lag by means of tsunami travel time charts, as was suggested by Mr. B. D. Zetler. The corrections for M2 are as follows: Canton Island 0 , Apra Harbor (Guam) 5 , Johnston Island 7 , Kwajalein 5 , Midway Island 4 , Tahiti 5 , Honolulu 5 . These phases are to be subtracted from the published M2 phases for these stations. Corrections for S2 and K1 are of similar small magnitude.

Larsen (1977) has shown how to remove the effect of extended island arcs (i.e., the Hawaiian Chain) from island tide observations. His method should be applied systematically in future refinements of the present study.

It should be noted that there is a growing set of coastal and deep sea pressure gauge measurements, which would provide an ideal data set for these calculations. At the present time, these measurements are being collected for publication under the auspices of the International Association for the Physical Sciences of the Ocean (IAPSO) by Cartwright and Zetler (Zetler, personal communication).

The M2 fit to observed tides for 3930 m mean depth plus scatter plots comparing it with island data are given in Figures 1 and 2. The least squares M2 elevation field shows structure similar to that of the solution of Zahel (1977). The main deviation occurs in the South Atlantic where Zahel shows an amphidrome not found in the least squares field. Otherwise, Zahel's amplitudes in the Pacific are significantly larger and his phases are entirely different there. The elevation field in the Atlantic and Indian Oceans is likewise similar to the corresponding cotidal charts of Dietrich (1944).

The S2 observed elevation field and corresponding scatter plots are given in Figures 3 and 4. It should be noted that the S2 tide includes significant radiational as well as gravitational forcing. Zetler (1971) indicates that the amplitude ratio between the radiational and gravitational tides off the coasts of the US is 16%. Since both the coastal and island elevations reflect this dual forcing, the least squares solution is expected to fit island data well even though the test functions were generated with only gravitational forcing.

The least squares K1 observed elevation field is similar to that of Dietrich (1944) throughout the world's oceans. The elevation field and its associated scatter plot are given in Figures 5 and 6.

Table 1 summarizes some features of the models, including the rate of working by the tide generating forces, the global average potential energy, and the global Q, all estimated as in Hendershott (1972); kinetic energy calculations involved unresolved numerical problems due to the proximity of the inertial latitudes to mesh points and hence equipartition was assumed. Platzman's (1975) results suggest that this involves an error of only a few percent.

The calculated rate of lunar working for the M2 model, 2.22×10^{19} erg s^{-1} , is smaller than the usual estimates, which range from 3.04×10^{19} erg s^{-1} for the Hendershott (1972) model to 3.77×10^{19} erg s^{-1} for Zahn (1977). This smaller value is in better agreement with the estimate of the M2 dissipation in shallow seas by Miller (1966) of 1.7×10^{19} erg s^{-1} . Astronomically generated estimates currently seem to be in a state of flux. Estimates recently have risen from the long accepted 2.7×10^{19} erg s^{-1} (derived from the Spencer-Jones value for the deceleration of the lunar longitude) and have subsequently fallen again. Muller (1976) reviews them

and places the present value at $3.3 \pm .2 \times 10^{19} \text{ erg s}^{-1}$. Goad and Douglas (1978) obtain a very similar value from analysis of satellite orbital parameters. It should be noted that this estimate represents the sum of all lunar dissipations, and as such should be considered simply an upper boundary for the M2 tide. Estimates of the non-M2 ocean effect on the lunar dissipation vary from $0.3-1.0 \times 10^{19} \text{ erg s}^{-1}$, thus reducing the above figure to $2.1-3.2 \times 10^{19} \text{ erg s}^{-1}$.

The nearness to resonance of the semi-diurnal constituents M2 and S2 makes it difficult to model these tides. The global Q values of 17.0 for M2 and 30.1 for S2 are consistent with the nearness to resonance. The K1 constituent on the other hand has every appearance of being far from resonance. The basic iterative procedure of Hendershott (1972) converges, and there is little difference between this solution and the least squares fit to island data. The only significant advantage of the fit to island data is that it better conserves mass. The apparent distance from resonance occurs despite the fact that Platzman (1975) finds several resonances near the diurnal frequency. No satisfactory explanation has been found. The calculated Q value for the island fit representation of 5.8 is consistent with the paradoxical absence of resonance.

4. MAPS OF THE GEOCENTRIC OCEAN TIDE, THE OCEAN INDUCED POTENTIAL, THE OCEAN INDUCED VERTICAL COMPONENT OF THE SOLID EARTH TIDE, AND THE OCEAN INDUCED GRAVITY TIDE

These maps are presented for their geophysical interest. The geocentric ocean tide $\zeta = \zeta_0 + \delta$ is directly observable by satellite altimetry. The total tide generating potential at the mean sea surface is

$$\Gamma = (1+k_2)U_2 + \Sigma(1+k'_n)g\alpha_n \zeta_{on},$$

the second half of this expression is the ocean induced potential at the mean sea surface. When analytically continued upward, $k_2U_2 + \Sigma(1+k'_n)g\alpha_n \zeta_{on}$ perturbs satellite orbits. It is not plotted since it may be obtained by adding k_2U_2 to the previous plot. The vertical solid earth tide is $\delta = h_2U_2/g + \Sigma h'_n \alpha_n \zeta_{on}$, the second half of this expression is the ocean induced vertical component of the solid earth tide. The ocean induced gravity tide as measured by a gravimeter on the solid earth's (moving) surface is

$$g/a \Sigma (n+2 h'_n - (n+1)k'_n) \alpha_n \zeta_{on}.$$

Here h'_n and k'_n are loading Love numbers (Munk and McDonald, 1960), $\alpha_n = (3/2n+1)(\text{water density/earth density})$, ζ_{on} is the n-th spherical harmonic of the observed ocean tide ζ_o , and a is the radius of the earth.

Note that the ocean induced potential at the solid earth's moving surface (i.e., not at mean sea level) is $\Sigma(1+k'_n - h'_n)g\alpha_n \zeta_{on}$. It is readily obtained by differencing the ocean induced potential at mean sea level and g times the ocean induced vertical component of the solid earth tide. It is therefore not plotted.

The maps are presented in Figures 7 through 18 in the order given in the title of this section. For each physical quantity the maps are in the order M2 then S2 then K1. Numerical tables of the mapped quantities are presented in a microfiche appendix available in limited supply from the office of Marine Geodesy.

It should be noted that these calculations do not include the ocean tides in coastal seas and shelves. Thus if one is interested in gravity or solid earth tides in a region near the coast, a local correction must be made using observations or reconstructions of nearby offshore tides.

All calculations were performed with Green's functions calculated by Farrell (1972).

Results of the K1 calculation are of particular interest because there is a proposed core resonance of near-K1 frequency (Rochester, 1973). Maps of the induced component of the gravitational field can therefore be used to indicate regions in which there is a likelihood that the K1 ocean contribution will be small; these then are optimum locations at which to look for the core resonance in gravity measurements. Indications are, from the calculations made here (Figure 18), that the best place for such measurements would be in Northern Russia where there is a large region with very small amplitudes evidently due to the great distance from the oceans. Because of the great extent of this region, positional errors should have little impact. The next most likely place would be in Australia where there appears to be an amphidrome. Unfortunately, the gradient away from the amphidrome is large, making correct placement of the amphidrome critical to finding the low amplitude region. In addition there is apparently an amphidrome in Antarctica, but as the core resonance signal dies off toward the pole, this may not be an optimal region for its measurement.

TABLE 1
ENERGETICS OF LEAST SQUARE TIDAL FIELDS

Model	n	Rate of working (ergs/sec)	Potential energy (ergs)	Q
M2 fit to island data	24	2.22×10^{19}	1.34×10^{24}	17.0
S2 fit to island data	16	2.08×10^{18}	2.15×10^{23}	30.1
K1 fit to island data	8	2.21×10^{18}	8.82×10^{22}	5.82

n represents the number of test functions used in the quasi-empirical fit

FIGURE CAPTIONS

- Figure 1. Dynamic interpolation of the global M2 tide based on test functions generated at 3930 m mean depth (amp. in cm, phases in degrees relative to passage of the tide generating body over Greenwich).
- Figure 2. Scatter diagrams comparing modeled M2 tidal elevations with island data.
- Figure 3. The same as Figure 1, except for S2.
- Figure 4. The same as Figure 2, except for S2.
- Figure 5. The same as Figure 1, except for K1.
- Figure 6. The same as Figure 2, except for K1.
- Figure 7. The geocentric M2 tide based on the model of Figure 1 (units as in Figure 1).
- Figure 8. The same as Figure 7, except based on the S2 model of Figure 3.
- Figure 9. The same as Figure 7, except based on the K1 model of Figure 5.
- Figure 10. The free space potential (divided by g) induced by the M2 model of Figure 1 (amp. in cm, phase in degrees as in Figure 1).
- Figure 11. The same as Figure 10, except induced by the S2 model of Figure 3.
- Figure 12. The same as Figure 10, except induced by the K1 model of Figure 5.
- Figure 13. The vertical component of the solid earth tide induced by the M2 model of Figure 1 (amp. in cm, phases in degrees as in Figure 1).

- Figure 14. The same as Figure 13, except induced by the S2 model of Figure 3.
- Figure 15. The same as Figure 13, except induced by the K1 model of Figure 5.
- Figure 16. The vertical component of the gravitational field induced by the M2 model of Figure 1 (amp. in 10^{-6} cm s⁻², phases in degrees as in Figure 1).
- Figure 17. The same as Figure 16, except induced by the S2 model of Figure 3.
- Figure 18. The same as Figure 16, except induced by the K1 model of Figure 5.

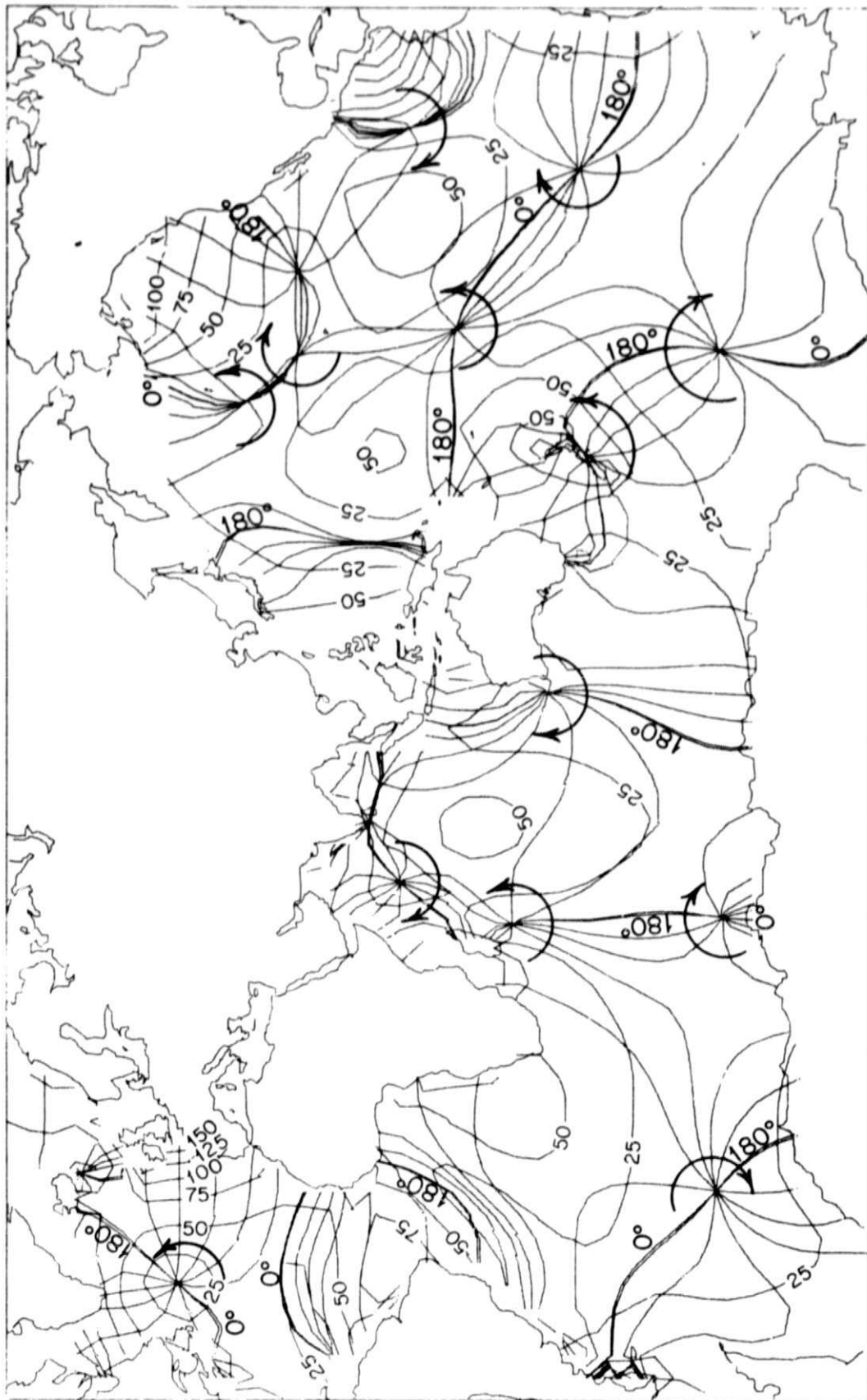


Figure 1.

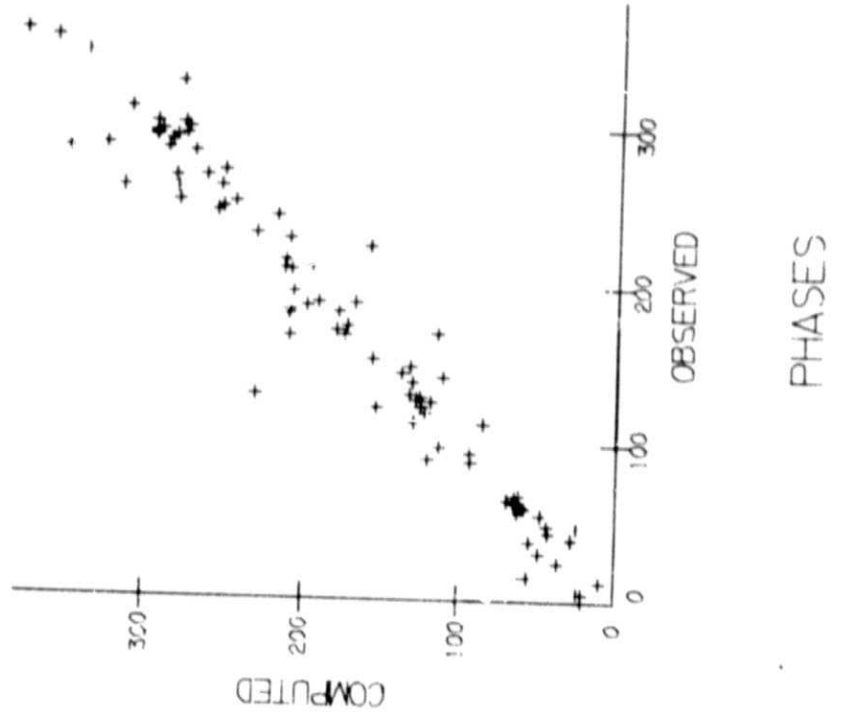
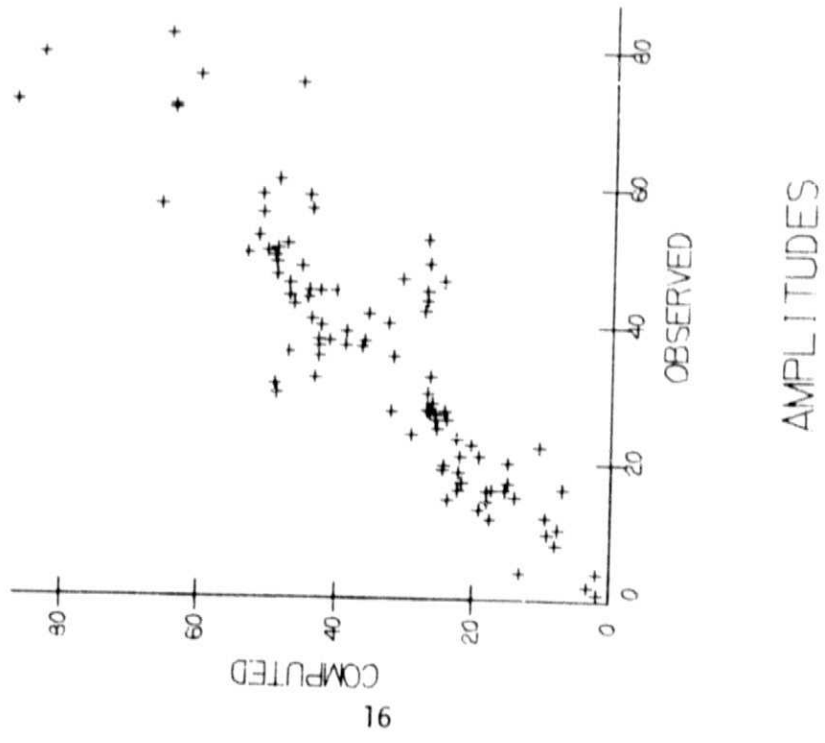


Figure 2.

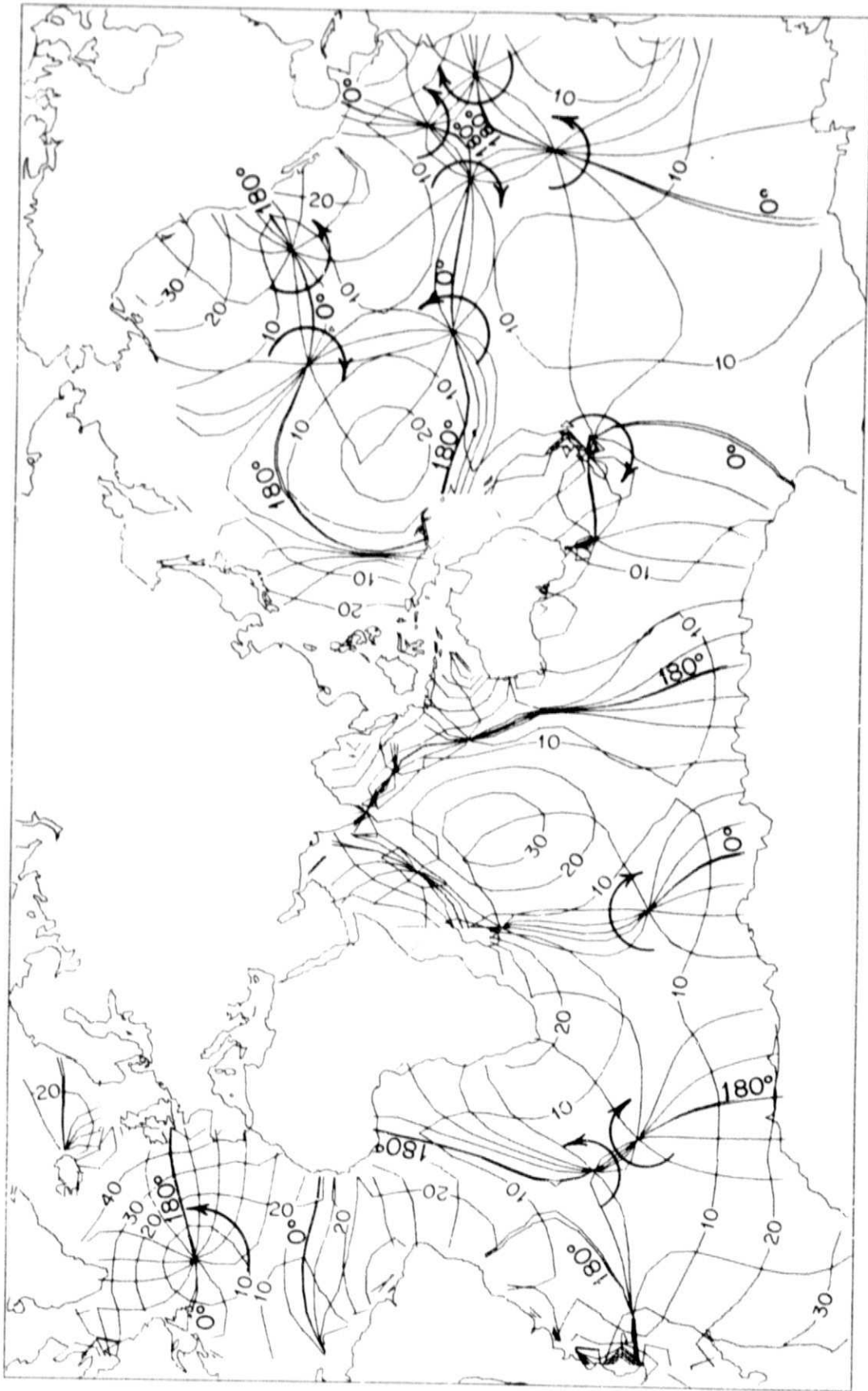


Figure 3.

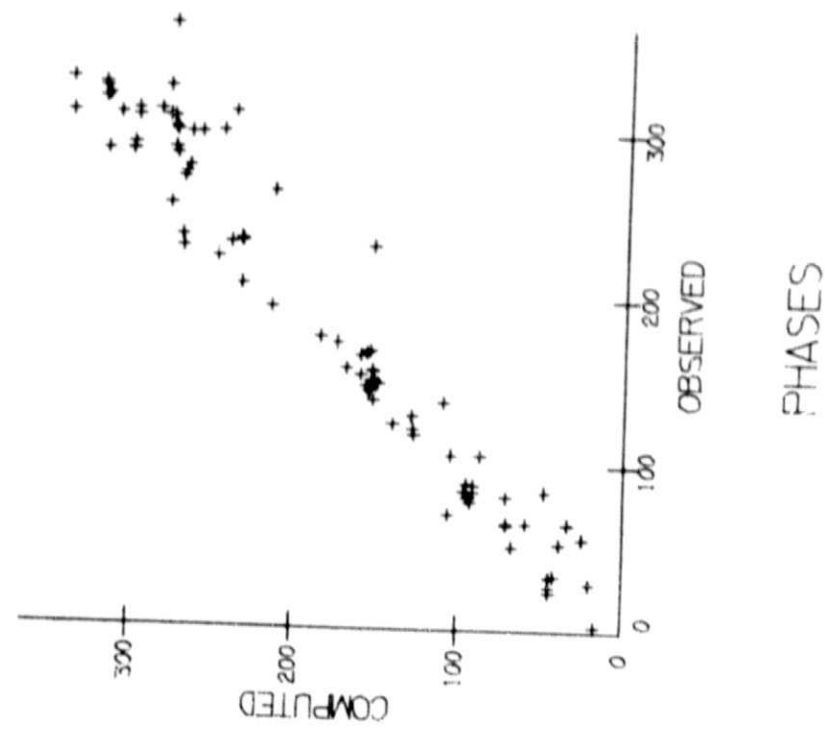
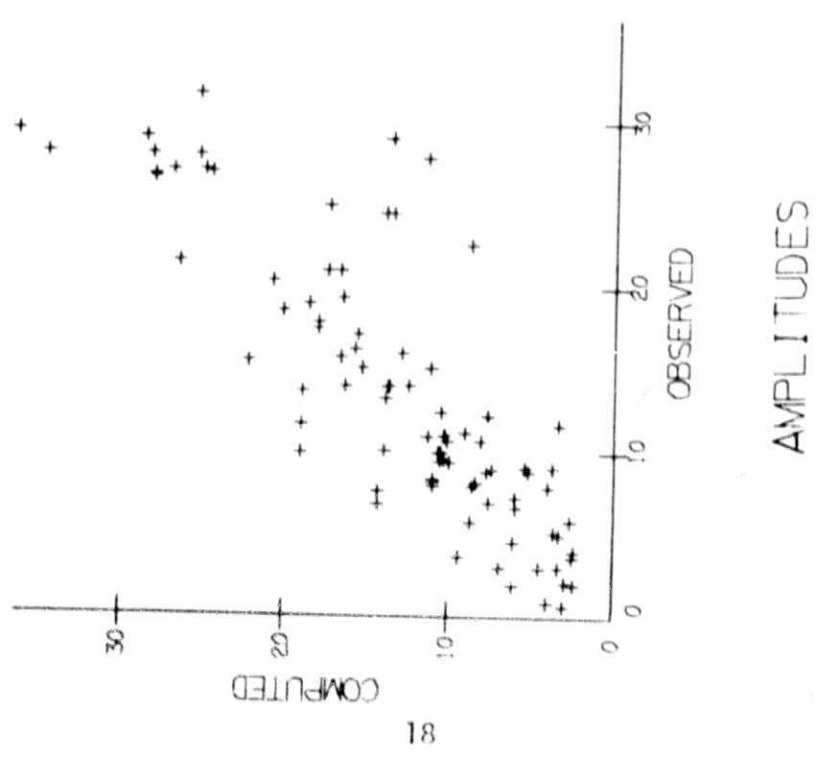


Figure 4.

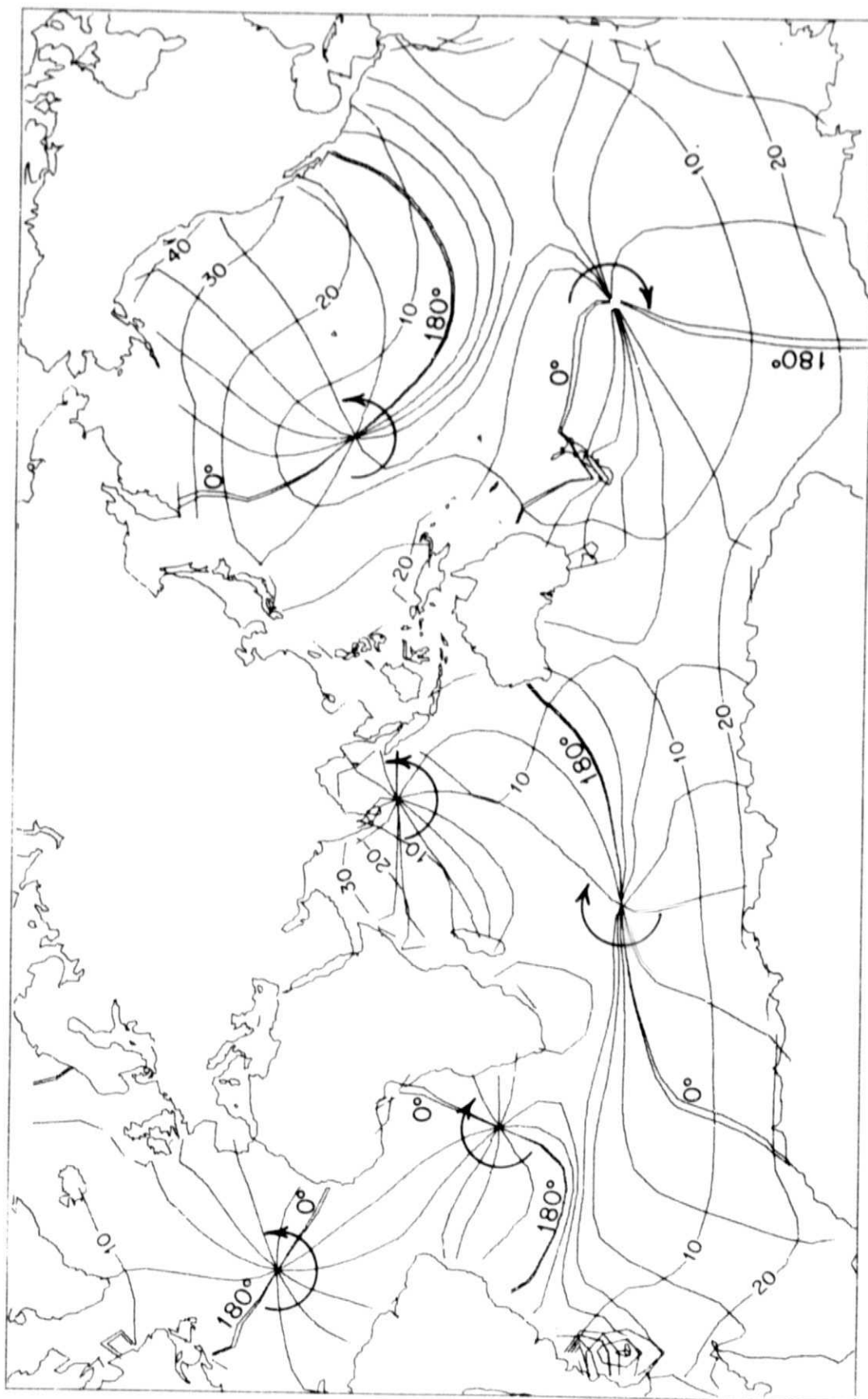
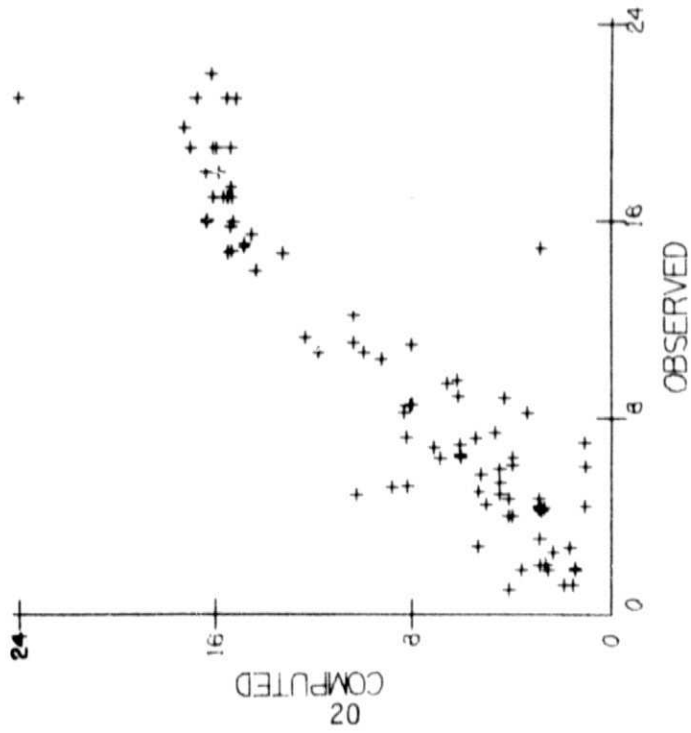
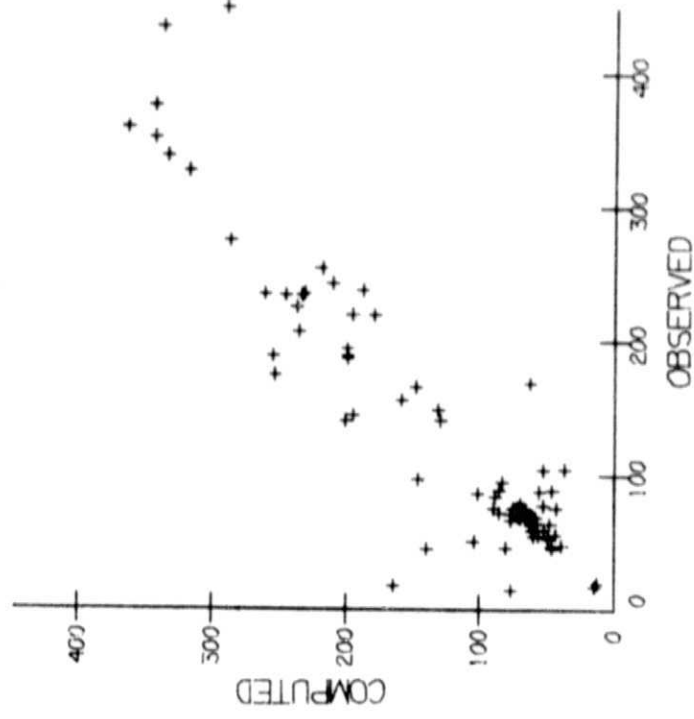


Figure 5.



AMPLITUDES



PHASES

Figure 6.

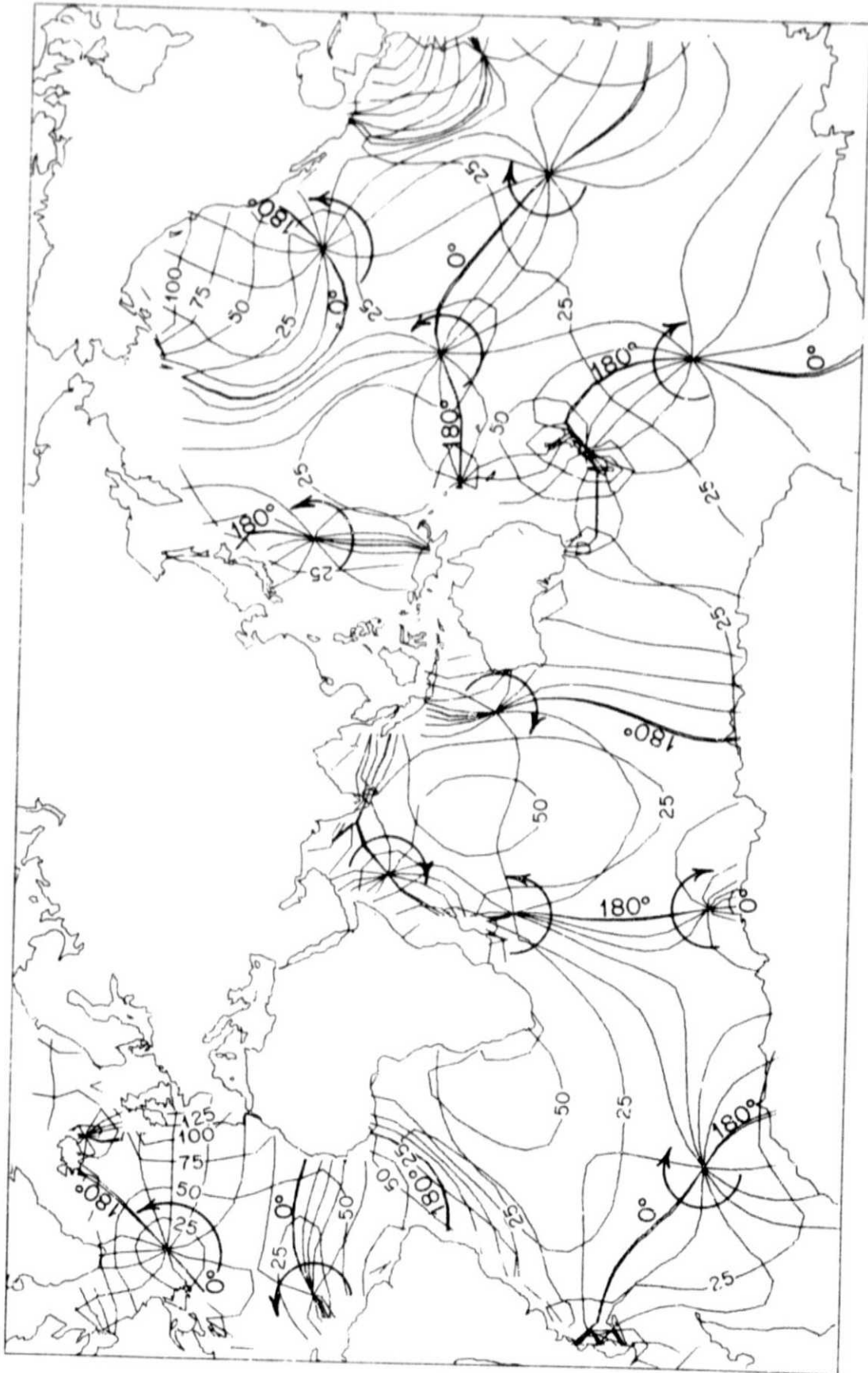


Figure 7.

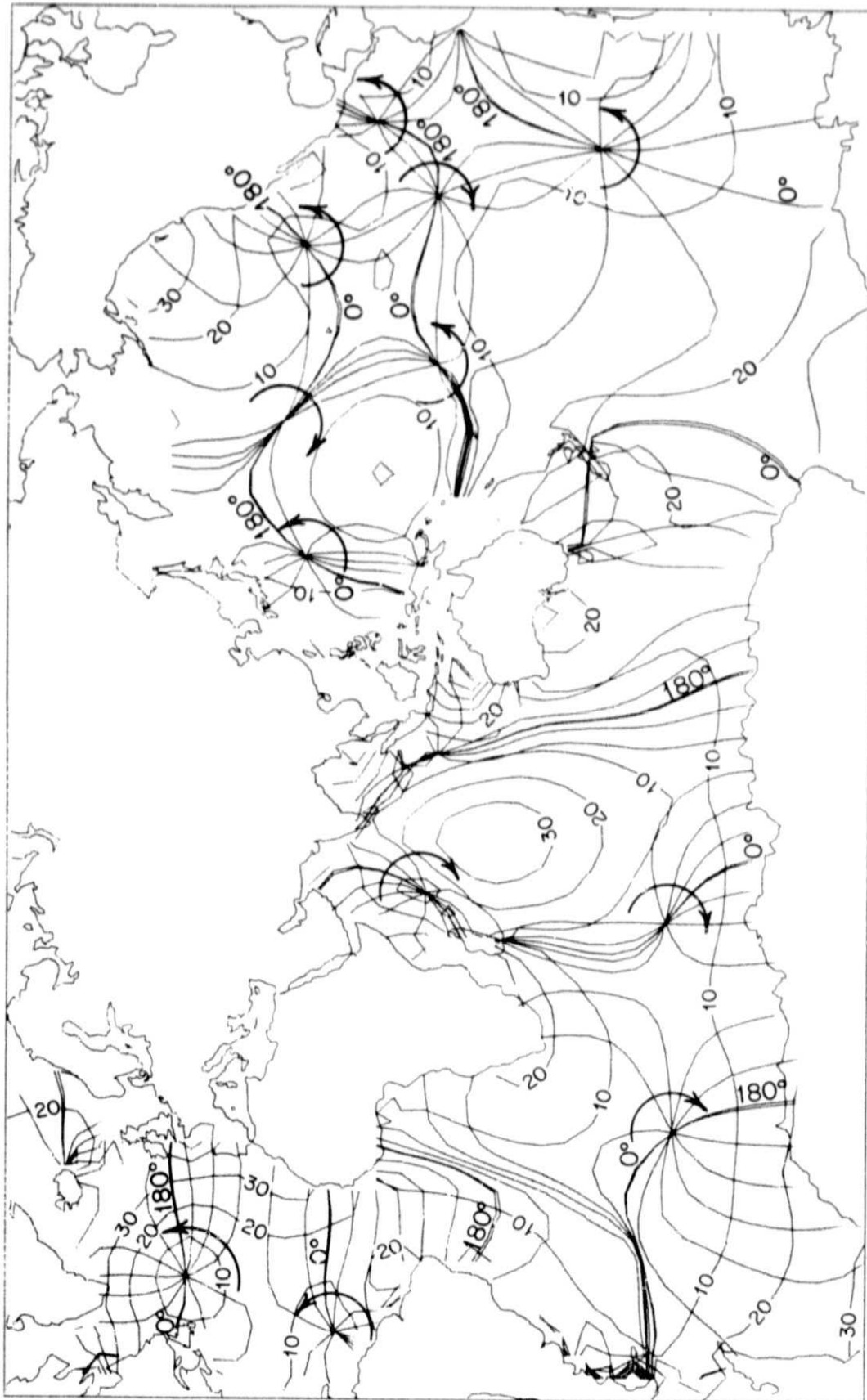


Figure 8.

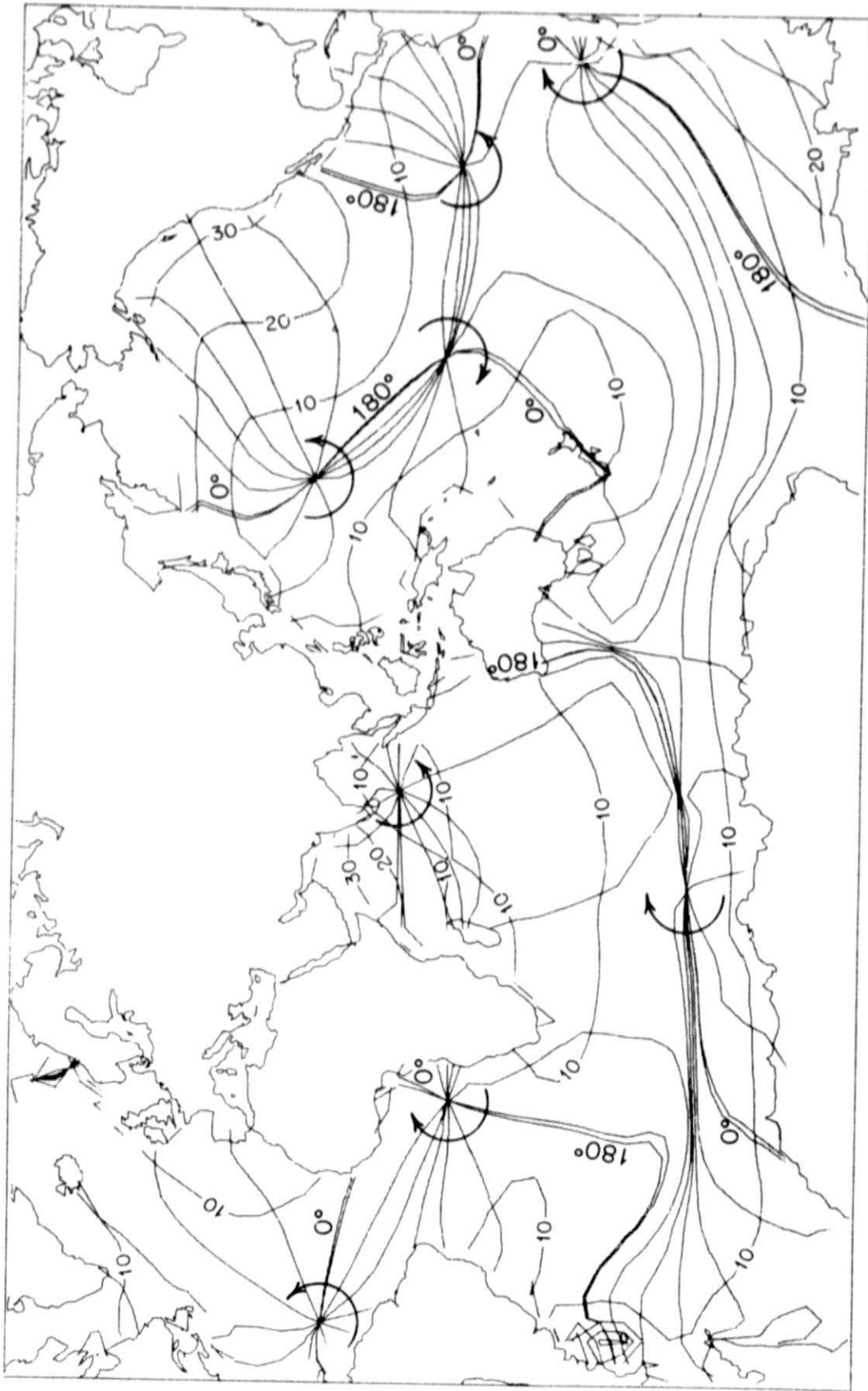


Figure 9.

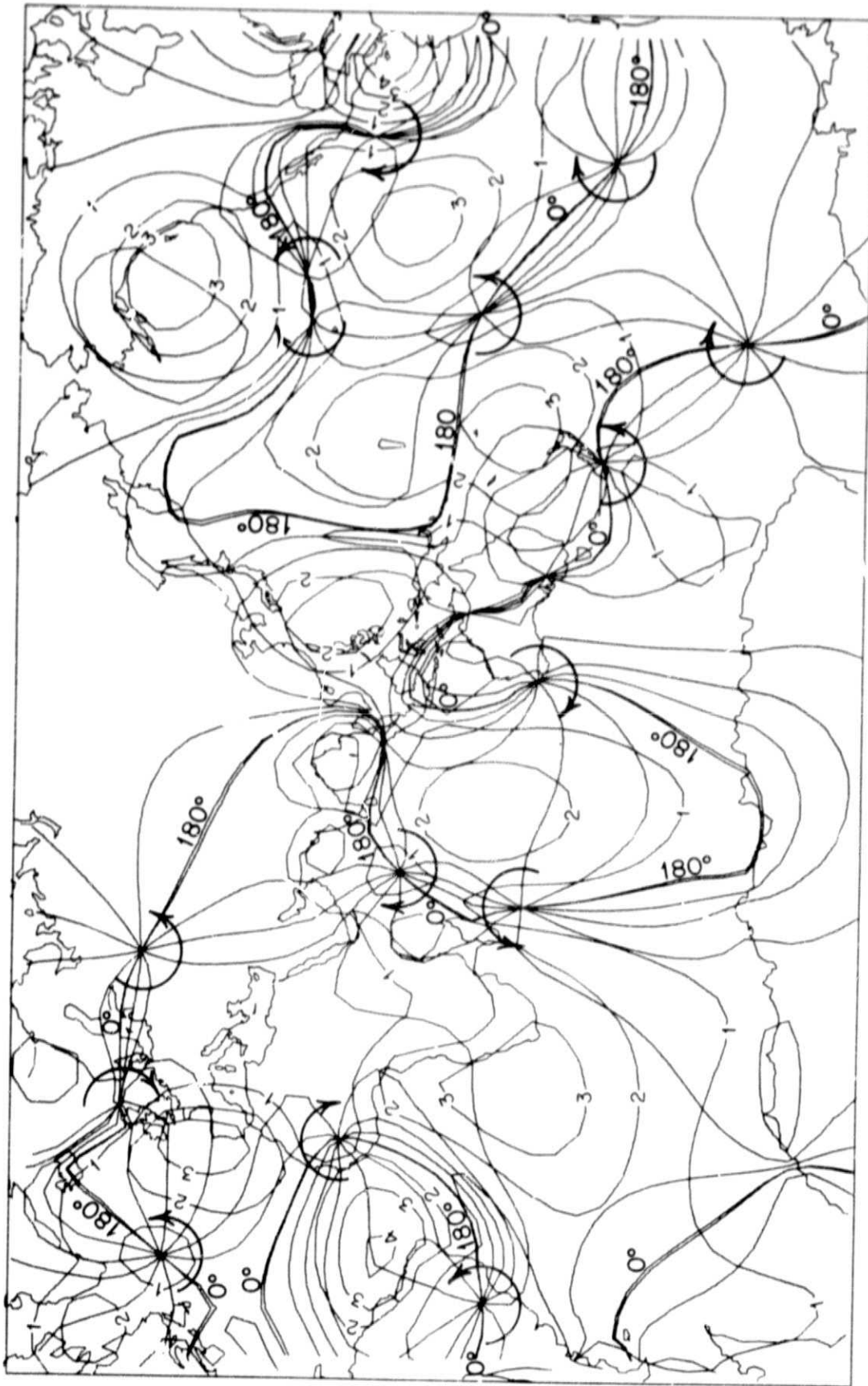


Figure 10.

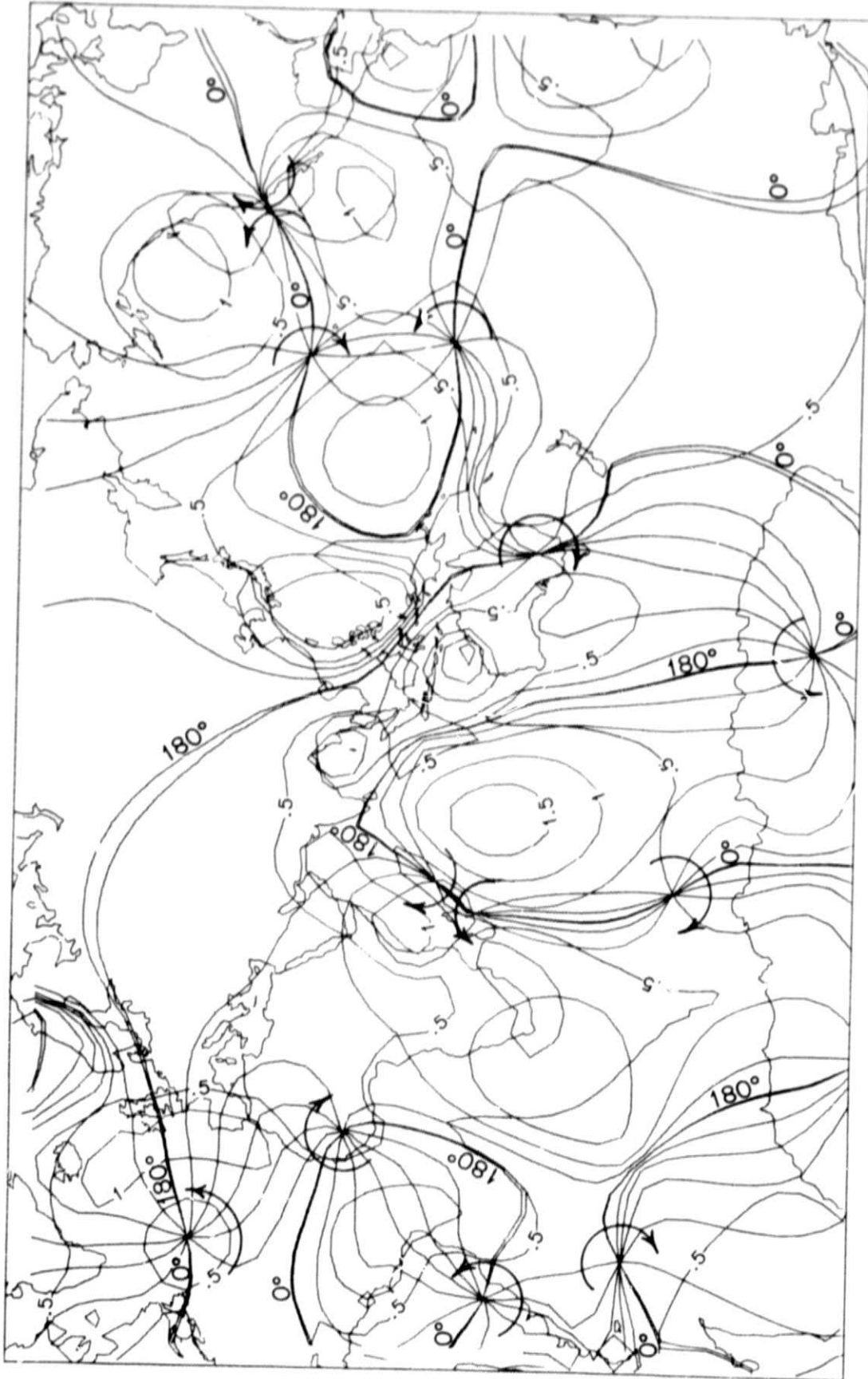


Figure 11.

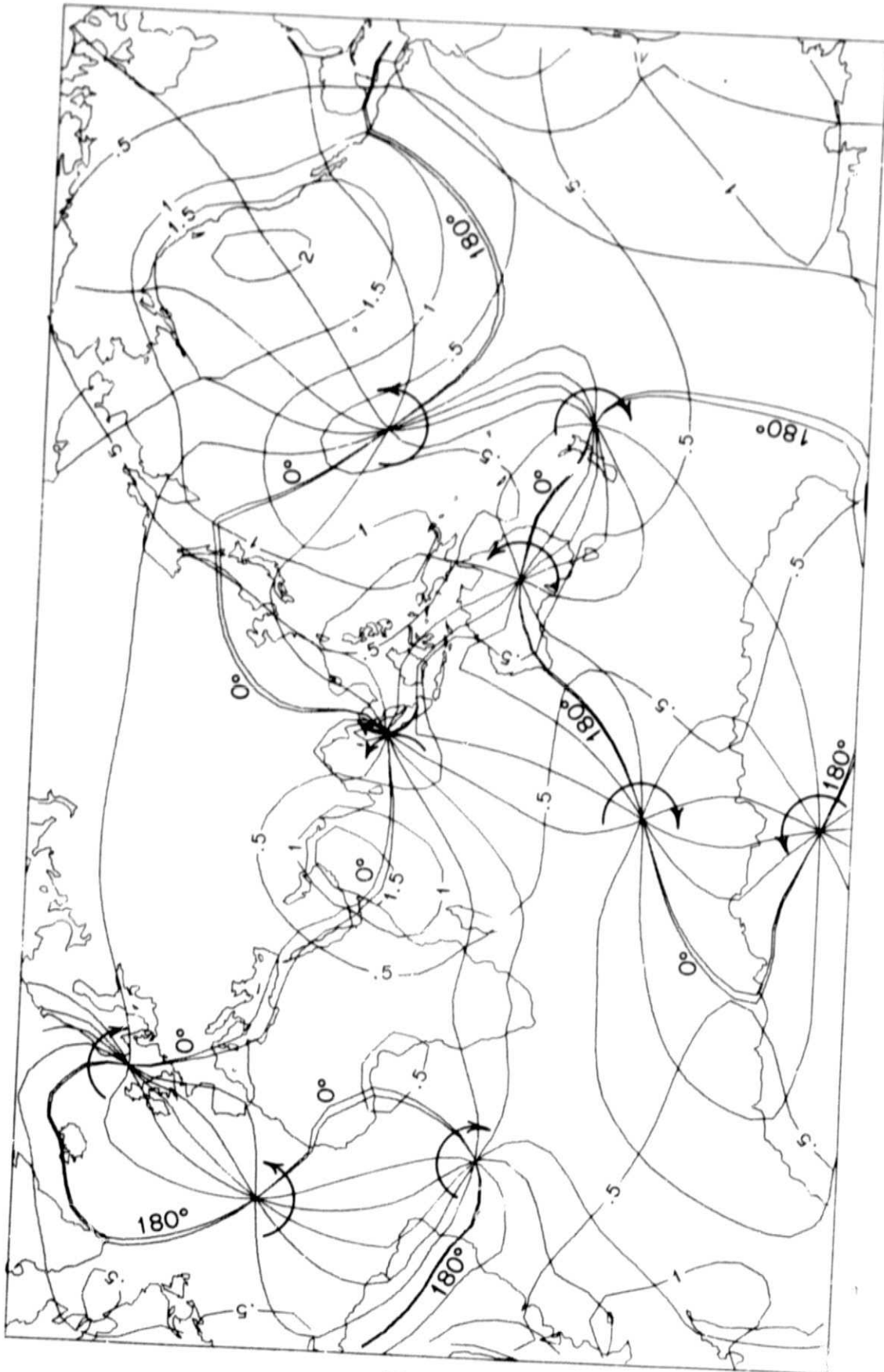


Figure 12.

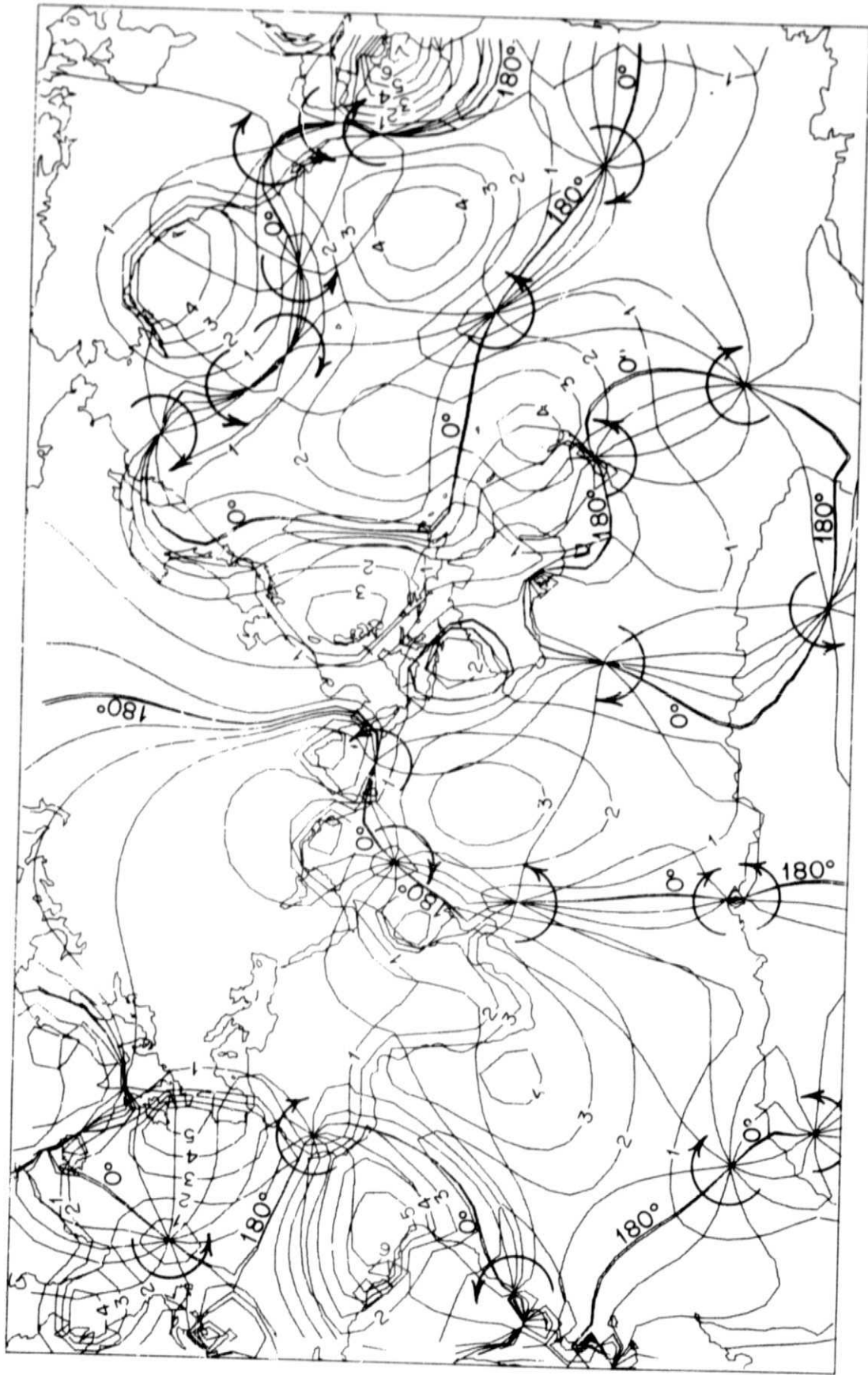


Figure 13.

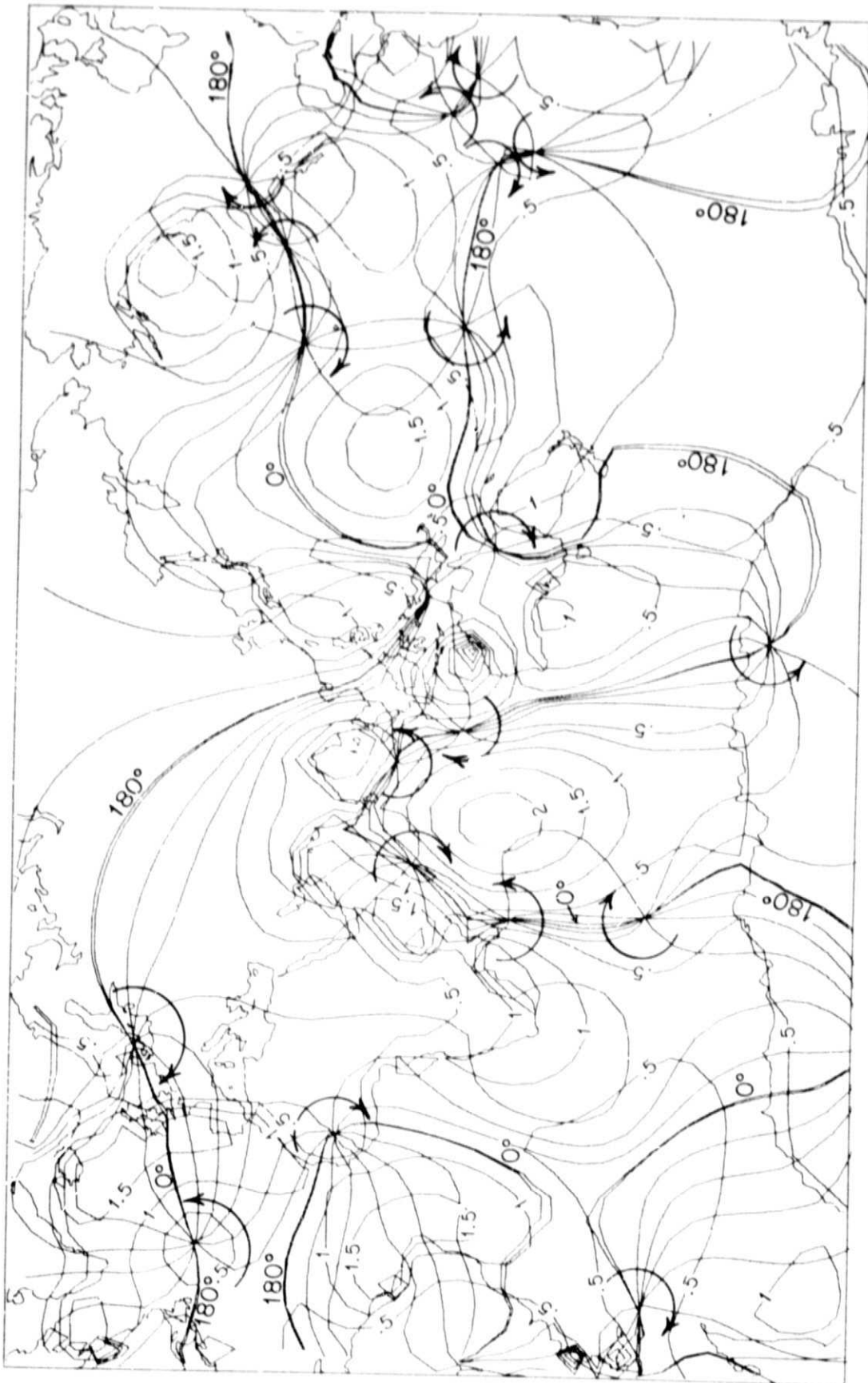


Figure 14.

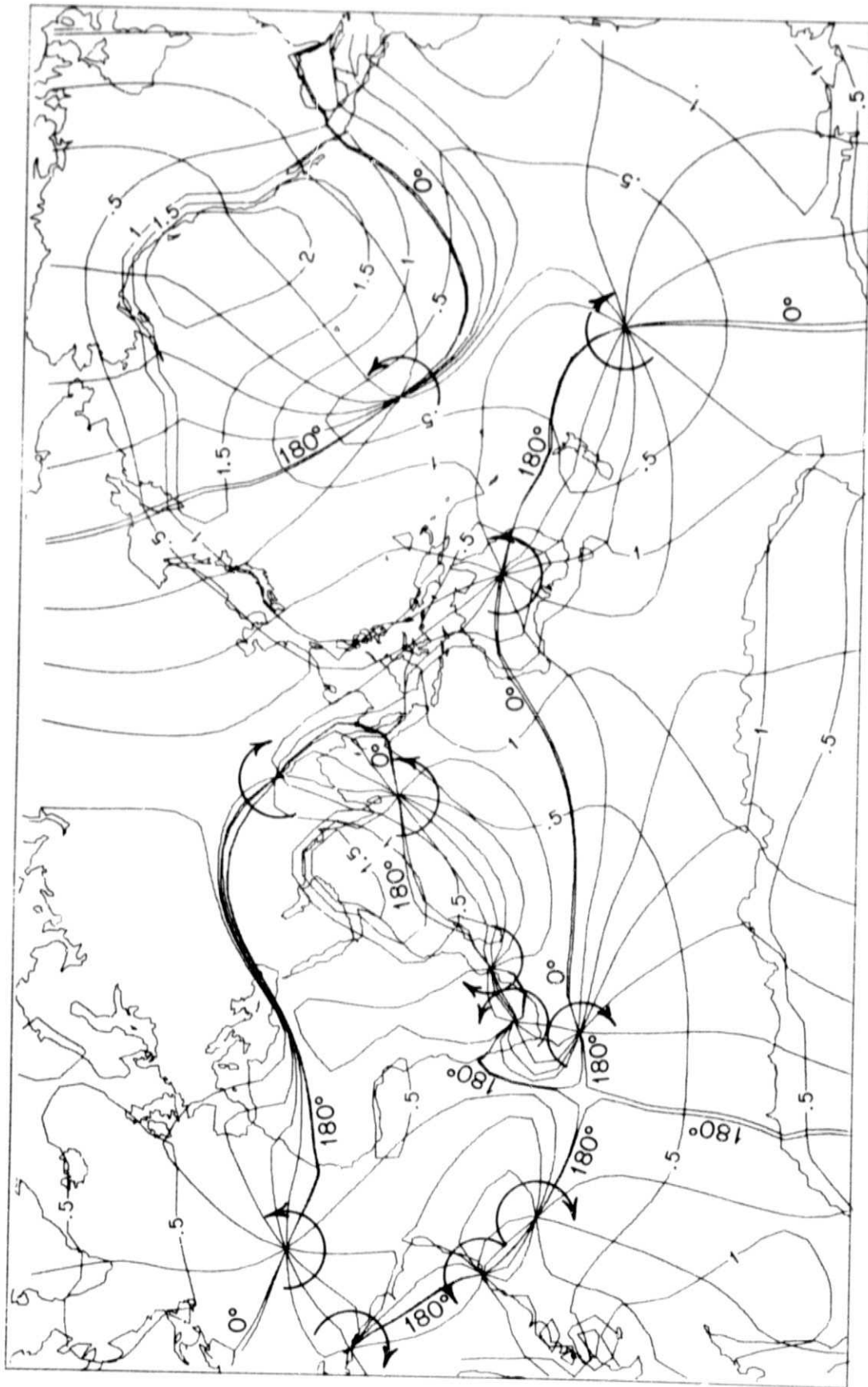


Figure 15.

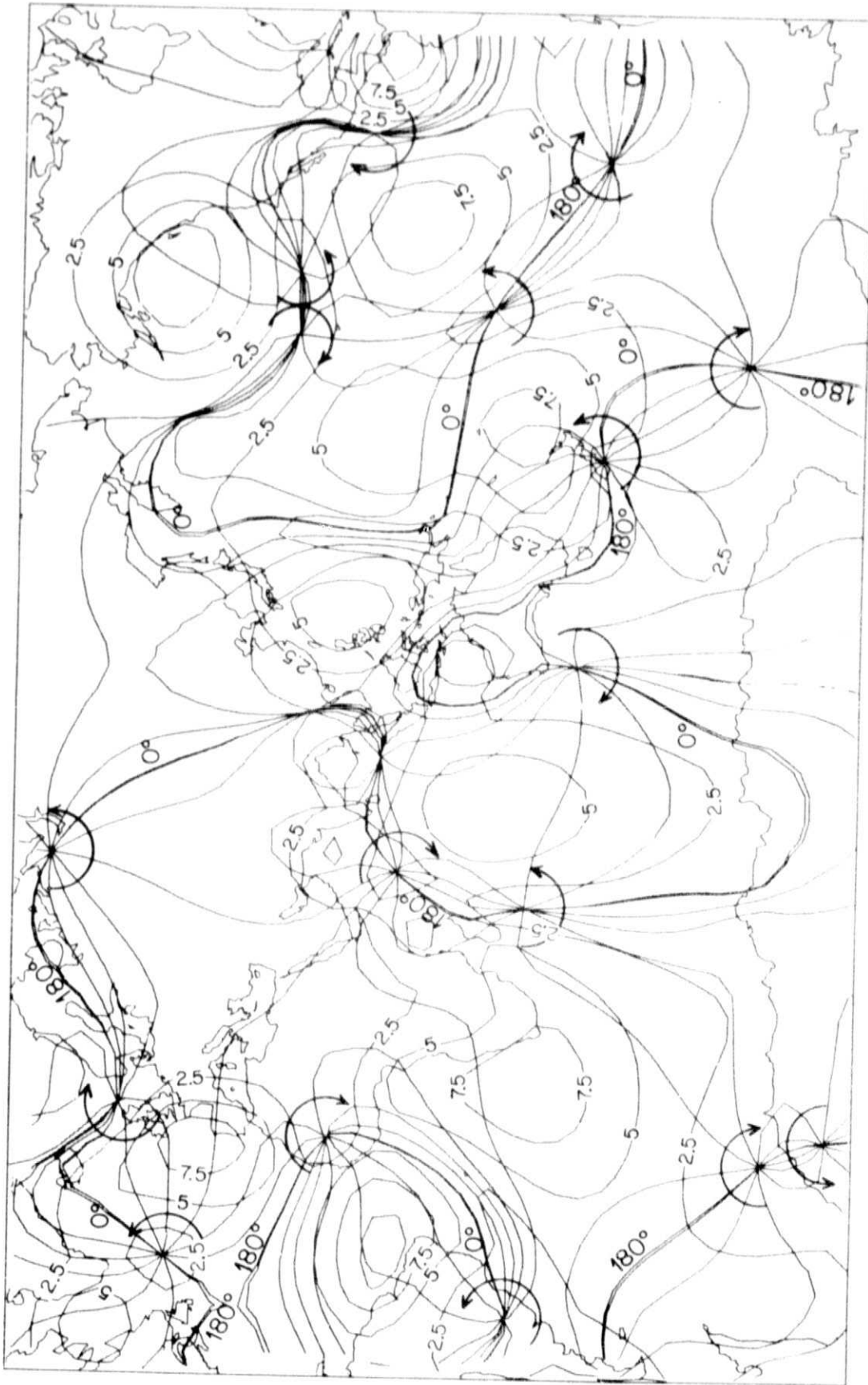


Figure 16.

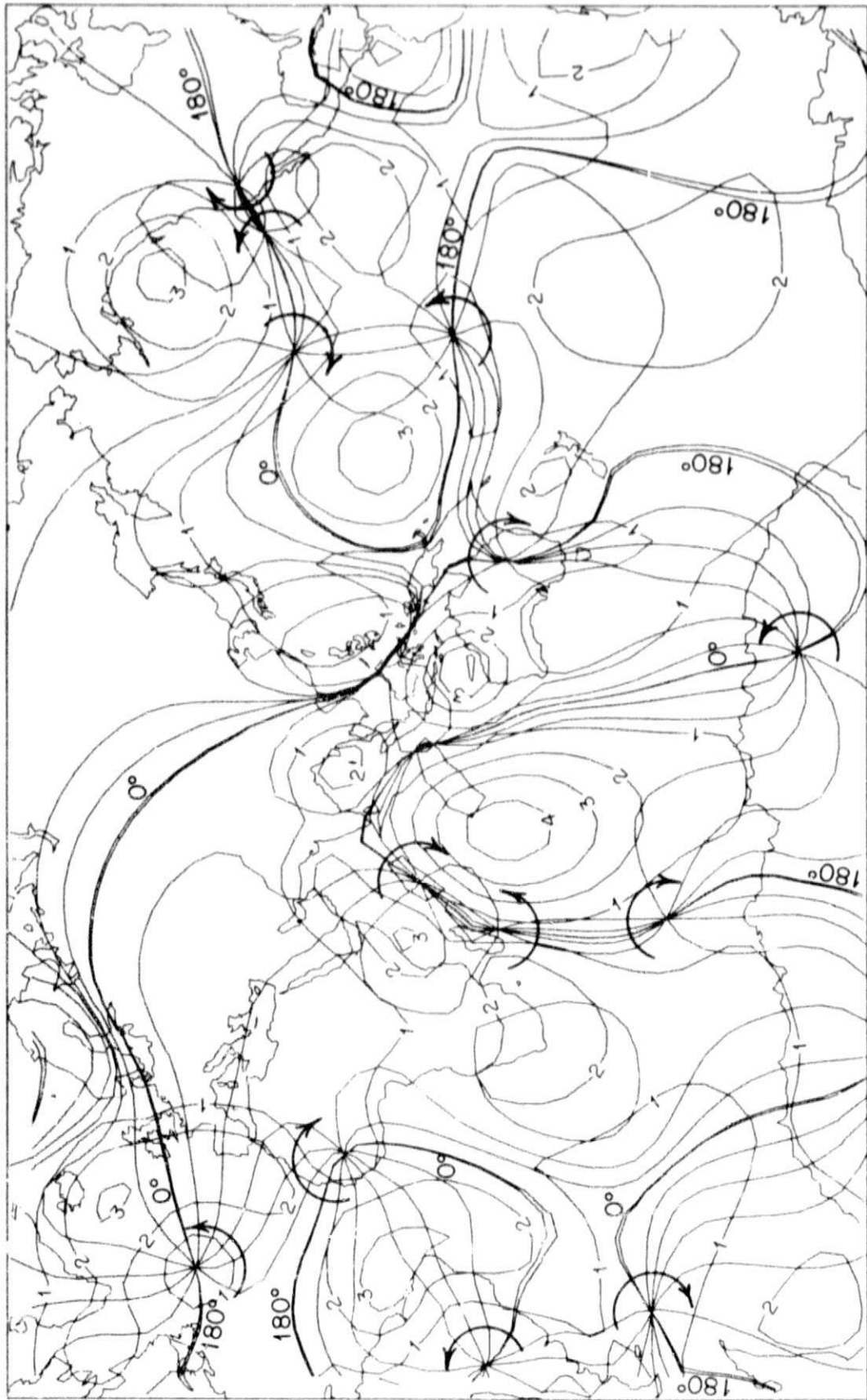


Figure 17.

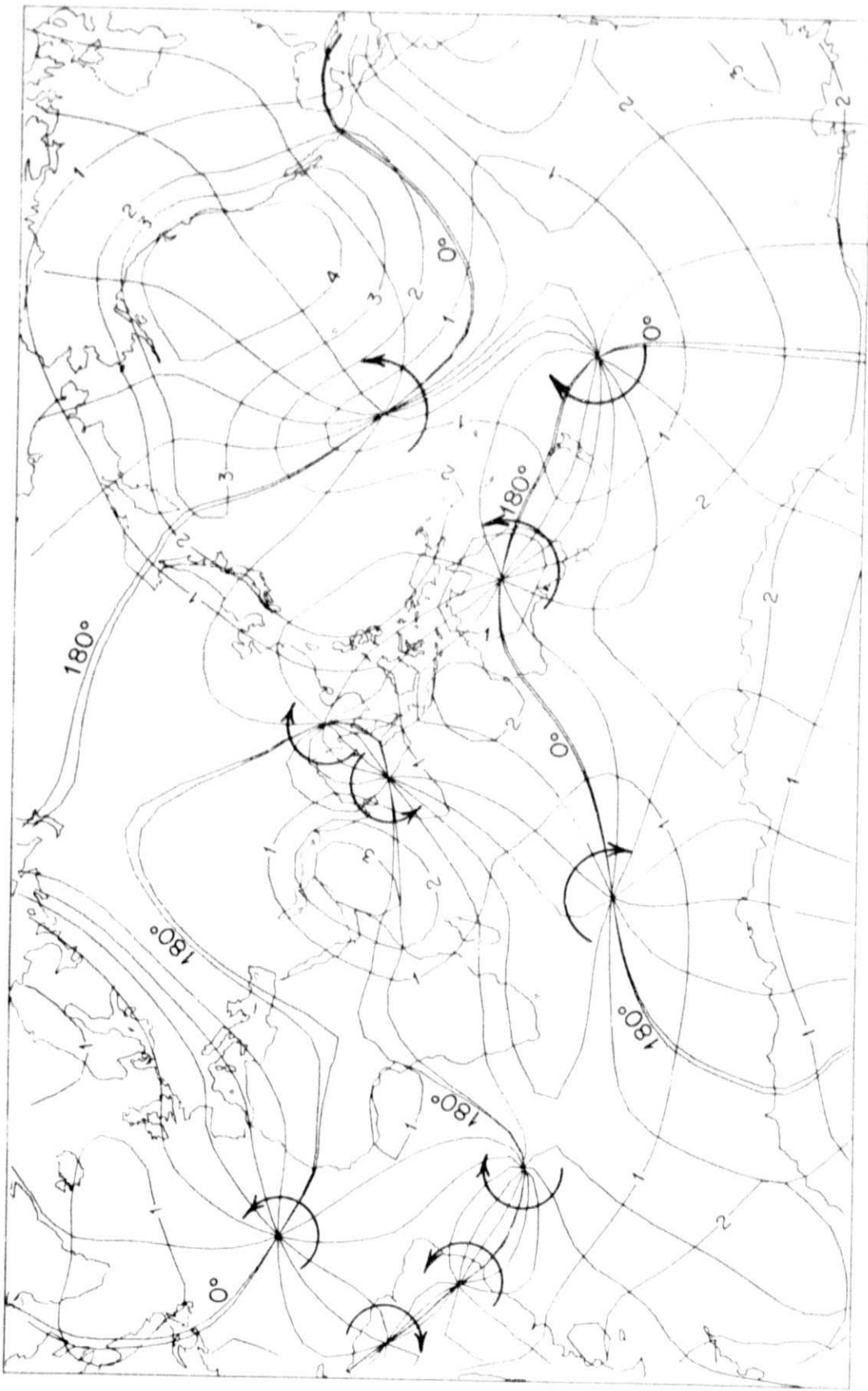


Figure 18.

References

- Backus, G., 1958, A class of self-sustaining dissipative spherical dynamos. *Annals of Physics*. (N.Y.), Vol. 4, pp. 372-447.
- Dietrich, G., 1944, Die Schwingungssysteme der halb- und eintagigen Tiden in den Ozeanen. *Veroeffentl. Inst. Meerskd. Univ. Berlin*, A, 41, pp. 7-68.
- Farrell, W. E., 1972, Deformation of the earth by surface loads. *Review of Geophysics and Space Physics*, Vol. 10, pp. 761-797.
- Goad, C. and Douglas, B., 1978, Lunar tidal acceleration obtained from satellite derived ocean tide parameters. *Journal of Geophysical Research*, Vol. 83, pp. 2306-2310.
- Gordeev, R., Kagan, A. and Polyakov, E., 1977. The effects of loading and self-attraction on global ocean tides, the model and the results of a numerical experiment. *Journal of Physical Oceanography*, Vol. 4, pp. 161-179.
- Hendershott, M. C., 1972, The effects of solid earth deformation on global ocean tides. *Geophysical Journal of the Royal Astronomical Society*, Vol. 29, pp. 389-402.
- Larsen, J., 1977. Cotidal charts for the Pacific Ocean near Hawaii using f-plane solutions. *Journal of Physical Oceanography*, Vol. 7, pp. 100-109.
- Miller, G., 1966, The flux of tidal energy out of the deep oceans. *Journal of Geophysical Research*, Vol. 71, pp. 2485-2489.
- Muller, P., 1976, Determination of the Rate of Change of G and the Tidal Acceleration of Earth and Moon from Ancient and Modern Astronomical Data. SP43-36, The Jet Propulsion Laboratory, Pasadena, California, 24 pages.
- Munk, W. H. and MacDonald, G., 1960, *The Rotation of the Earth*. Cambridge University Press, London.
- Parke, M. E., 1978, Global numerical models of the open ocean tides M2, S3, K1 on an elastic earth. PhD Thesis, Univ. of California, San Diego.
- Platzman, G.W., 1975, Normal modes of the Atlantic and Indian Oceans. *Journal of Physical Oceanography*, Vol. 5, pp. 201-221.
- Rochester, M. G., 1973, *The Earth's Rotation*. Transactions of the American Geophysical Union, Vol. 54, pp. 769-780.
- Stock, G., 1976, Modelling of tides and tidal dissipation in the Gulf of California. PhD Thesis, Univ. of California, San Diego.
- Zahel, W., 1977, A global hydrodynamic-numerical model of the ocean tides. Proceedings of the IRIA International Colloquium on Numerical Methods of Science and Technical Computations (Berlin; Springer Verlag).
- Zetler, B., 1971, Radiational ocean tides along the coasts of the United States. *Journal of Physical Oceanography*, Vol. 1, pp. 34-38.